

New method to detect rotation in high-energy heavy-ion collisions

L. P. Csernai,¹ S. Velle,¹ and D. J. Wang^{1,2}¹*Institute of Physics and Technology, University of Bergen, Allegaten 55, 5007 Bergen, Norway*²*Key Laboratory of Quark and Lepton Physics (MOE) and Institute of Particle Physics, Central China Normal University, Wuhan 430079, China*

(Received 6 May 2013; revised manuscript received 18 October 2013; published 31 March 2014)

With increasing beam energies the angular momentum of the fireball in peripheral heavy-ion collisions increases, and the proposed differential Hanbury Brown and Twiss analysis is able to estimate this angular momentum quantitatively. The method detects specific space-time correlation patterns, which are connected to rotation.

DOI: [10.1103/PhysRevC.89.034916](https://doi.org/10.1103/PhysRevC.89.034916)

PACS number(s): 25.75.Gz, 25.75.Nq

I. INTRODUCTION

In high-energy peripheral heavy-ion collisions a high angular momentum is realized in rotating flow, large velocity shear, vorticity, and circulation. Viscous, explosive expansion leads to a decrease in vorticity and circulation with time, however, with small viscosity the vorticity remains significant at the final freeze-out (FO) stages. The proposed differential Hanbury Brown and Twiss (HBT) analysis, a combination of standard two-particle correlation functions, is adequate to analyze rotating systems. At the present collision energies the angular momentum and rotation are becoming a dominant feature of reaction dynamics, and up to now the rotation of the system has not been analyzed, either with the HBT method or in any other way. We present and analyze this method and its results in a high-resolution, particle-in-cell fluid dynamics model. Fluid dynamics is proven to be the best theoretical method to describe collective flow phenomena. The same model was used to predict the rotation in peripheral ultrarelativistic reactions [1], to point out the possibility of Kelvin Helmholtz instability (KHI) [2], flow vorticity [3], and polarization arising from local rotation, i.e., vorticity [4]. The model was also tested for its numerical viscosity and the resulting entropy production [5]. The formation of KHI was also observed recently in AdS/CFT holography, where the instability is even more pronounced in peripheral reactions, although the time scale is sufficiently short only at high quark chemical potentials as at FAIR, NICA, and RHIC-BES [6].

The total angular momentum of the fireball is maximal at $b = 0.3b_{\max}$ [7], while the angular momentum per net baryon charge is maximal around $b = (0.5-0.8)b_{\max}$. At ultraperipheral collisions fluctuations dominate collective effects. According to the present analysis the differential HBT method indicates rotation via particles at collective momenta, $p_t \approx (0.5-2)$ GeV/c the best, and the magnitude of the introduced differential correlation function (DCF) increases monotonically with the angular momentum.

II. CORRELATION FUNCTION FROM FLUID DYNAMICS

The pion correlation function is defined as the inclusive two-particle distribution divided by the product of the inclusive

one-particle distributions, such that [8]

$$C(p_1, p_2) = \frac{P_2(p_1, p_2)}{P_1(p_1)P_1(p_2)}, \quad (1)$$

where p_1 and p_2 are the four-momenta of pions. We introduce the center-of-mass (c.m.) momentum, $^1k = \frac{1}{2}(p_1 + p_2)$, and the relative momentum, $q = p_1 - p_2$, where from the mass-shell condition [8] $q^0 = \mathbf{k}q/k^0$. We use a method for moving sources presented in Ref. [9],

$$C(k, q) = 1 + \frac{R(k, q)}{|\int d^4x S(x, k)|^2}, \quad (2)$$

where

$$R(k, q) = \int d^4x_1 d^4x_2 \cos[q(x_1 - x_2)] \times S(x_1, k + q/2) S(x_2, k - q/2). \quad (3)$$

Using the emission function $S(x, k)$, discussed in Ref. [10], here $R(k, q)$ can be calculated [9] via the function

$$J(k, q) = \int d^4x S(x, k + q/2) \exp(iqx), \quad (4)$$

and we obtain the $R(k, q)$ function as $R(k, q) = \text{Re} [J(k, q) J(k, -q)]$.

We estimate the local pion density by the specific entropy, $\sigma(x)$, as $n_\pi(x) \propto n(x) \sigma(x)$, where $n(x)$ is the proper net baryon charge density.² Thus the local invariant pion density is given by the Jüttner distribution as

$$f^J(x, p) = \frac{n(x)\sigma(x)}{C_\pi} \exp\left(-\frac{p^\mu u_\mu(x)}{T(x)}\right), \quad (5)$$

¹The vector \mathbf{k} is the wave-number vector $\mathbf{k} = \mathbf{p}/\hbar$, so for numerical calculations we have to use that $\hbar c = 197.327$ MeV fm. The same applies to \mathbf{q} .

²At the latest times presented here, $t = 3.56$ fm/c (~ 8 fm/c after the initial touch), the net baryon density is sufficiently high at nonvanishing entropy, so this approximation is satisfactory. At later times the entropy density becomes dominant, while the net baryon density decreases.

where $C_\pi = 4\pi m_\pi^2 T K_2(m_\pi/T)$ at temperature T , and K_2 is a modified Bessel function.

We assume that the single-particle distributions, $f(x, p)$, in the source functions are Jüttner distributions, which depend on the local velocity, $u^\mu(x)$, and we use the notation $u_1 = u(x_1) = u^\mu(x_1)$.

Using the Cooper-Frye FO description we can connect the Source function, S , to the phase space distribution function on the FO hypersurface. Let the space-time (ST) points of the hyper-surface be given in parametric form $x_{\text{FO}} = x_{\text{FO}}(x)$, which can be given by the FO condition (e.g., $t = \text{const.}$, $\tau = \text{const.}$, $T = \text{const.}$). In the source function formalism this corresponds to a four-volume integral,

$$\begin{aligned} \int d^4x S(x, p) &= \int d^4x f^J(x, p) P(x, p) \\ &= \int d^4x f^J(x, p) \delta(x - x_{\text{FO}}) p^\mu \hat{\sigma}_\mu, \end{aligned}$$

where the emission probability is [11] $P(x, p) = \delta(x - x_{\text{FO}}) p^\mu \hat{\sigma}_\mu$. This Cooper-Frye FO treatment is the most frequent in fluid dynamical models. This sudden FO assumption can be relaxed by assuming an extended FO layer in space time via replacing the Dirac δ function with an FO profile function in $P(x, p)$, e.g.,

$$\begin{aligned} P(x, p) &= \delta(x - x_{\text{FO}}) p^\mu \hat{\sigma}_\mu \\ &\rightarrow \frac{1}{\sqrt{\Delta\pi}} \exp\left(-\frac{(s - s_{\text{FO}})^2}{\Delta}\right) p^\mu \hat{\sigma}_\mu, \end{aligned}$$

where s is a local coordinate in the direction of $\hat{\sigma}^\mu$, and the local width of the FO layer is $\Delta = \Delta(x)$ (which should tend to 0 to get the Dirac δ function for the emission probability). This description is then completely general, with the only assumption that the emission probability has a Gaussian profile. (This could also be relaxed.)

If we assume that the two coincident particles originate from two points, x_1 and x_2 , the expression of the correlation function, Eq. (3), will become [10]

$$\begin{aligned} R(k, q) &= \int d^4x_1 d^4x_2 S(x_1, k) S(x_2, k) \cos[q(x_1 - x_2)] \\ &\times \exp\left[-\frac{q}{2} \cdot \left(\frac{u(x_1)}{T(x_1)} - \frac{u(x_2)}{T(x_2)}\right)\right], \end{aligned} \quad (6)$$

and the corresponding $J(k, q)$ function is

$$J(k, q) = \int d^4x S(x, k) \exp\left[-\frac{q \cdot u(x)}{2T(x)}\right] \exp(iqx). \quad (7)$$

In Ref. [10] different one-, two-, and four-source systems were tested with and without rotation. Here we study only the case where the emission is *asymmetric* and dominated by the fluid elements facing the detector.

In numerical fluid dynamical studies of symmetric (A + A) nuclear collisions the initial state is symmetric around the c.m. of the system, and (if we do not consider random fluctuations) this symmetry is preserved during the fluid dynamical evolution. Let us consider the usual conventions, z is the beam axis, and the positive z direction is the direction

of the projectile beam. The impact parameter vector points into the positive x direction, i.e., towards the projectile. Finally, the y axis is orthogonal to both.

The fluid dynamical system, without fluctuations, can be considered as a set of symmetric pairs of fluid cells. The emission probabilities for the two fluid cells of a source pair are not equal.

If we have several fluid cell sources, s , with Gaussian ST emission profiles, then the source function in the Jüttner approximation is

$$\begin{aligned} \int d^4x S(x, k) &= \sum_s \int_s d^3x_s dt_s S(x_s, k) \\ &= (2\pi R^2)^{3/2} \sum_s \frac{\gamma_s n_s(x) (k_\mu \hat{\sigma}_s^\mu)}{C_s} \\ &\times \exp\left[-\frac{k \cdot u_s}{T_s}\right], \end{aligned} \quad (8)$$

where $n_s = n_\pi$, and the spatial integral over a cell volume is, $V_{\text{cell}} = (2\pi R^2)^{3/2}$, while the time integral is normalized to unity. Similarly, the J function is

$$J(k, q) = \sum_s e^{-\frac{q \cdot u_s}{2T_s}} e^{iqx_s} \int_s d^4x S_s(x, k) e^{iqx}. \quad (9)$$

We then assume that the FO layer is relatively narrow compared to the spatial spread of the fluid cells, so that the peak emission times, t_s , of all fluid cells are the same. Then the $\exp(iq^0 t_s)$ factor drops out from the $J(k, q)J(k, -q)$ product.³ This FO simplification is justified for rapid and simultaneous hadronization and FO from the plasma. For dilute and transparent matter the correlations from the time dependence of FO should be handled the same way as the spatial dependence.

Due to mirror symmetry with respect to the $[x, z]$ reaction plane, it is sufficient to describe the cells on the positive side of the y axis. The other side is the mirror image of the positive side. Then we can evaluate the correlation function the same way as in Ref. [10].

Thus we define the quantities

$$\begin{aligned} Q_c &= (2\pi R^2)^{3/2} \exp\left[-\frac{R^2 q^2}{2}\right], \\ P_s &= \frac{\gamma_s n_s}{C_s} \exp\left[-\frac{k_0 u_s^0}{T_s}\right], \\ Q_s^{(q)} &= \exp\left[-\frac{q_0 u_s^0}{2T_s}\right], \\ w_s &= (k_\mu \hat{\sigma}_s^\mu) \exp\left[-\frac{\Theta_s^2}{2} q_0^2\right], \end{aligned} \quad (10)$$

³If the emission is happening through a layer with a time-like normal, but the peak is not at a constant t_s but, rather, at a constant τ_s , then we can adapt the coordinate system accordingly; i.e., we can use the τ, η coordinates instead of t, z (see, e.g., [11]).

where $u_s^0 = \gamma_s$, the local four-direction normal of the mean particle emission from an ST point of the flow is $\hat{\sigma}_s^\mu$ (assumed to be time-like), R is the size (radius) of the fluid cells, and Θ_s is the path length of the time integral from the ST point of the source, s , while assuming a Gaussian emission time profile [10]. The weights w_s arise directly from the Cooper-Frye formula [11].

We can reassign the summation for pairs, so that $s = \{i, j, k\}$ will correspond to a pair of cells at $\{i, j, k\}$ and its reflected pair across the c.m. point at the same time at $\{i^*, j^*, k^*\}$. Then the function $S(k, q)$ becomes

$$\begin{aligned} & \int d^4x S(x, k) \\ &= (2\pi R^2)^{3/2} \sum_s P_s \left[w_s \exp\left(\frac{\mathbf{k}u_s}{T_s}\right) + w_s^* \exp\left(\frac{\mathbf{k}u_s^*}{T_s}\right) \right], \end{aligned} \quad (11)$$

while the function $J(k, q)$ becomes

$$\begin{aligned} J(k, q) &= Q_c \sum_s P_s \left[Q_s^{(q)} w_s \exp\left[\left(\mathbf{k} + \frac{\mathbf{q}}{2}\right) \frac{u_s}{T_s}\right] e^{iqx_s} \right. \\ &\quad \left. + Q_s^{(q)} w_s^* \exp\left[\left(\mathbf{k} + \frac{\mathbf{q}}{2}\right) \frac{u_s^*}{T_s}\right] e^{iqx_s^*} \right]. \end{aligned}$$

Only the mirror symmetry across the participant c.m. is assumed, which is always true for globally symmetric, A + A, heavy-ion collisions in a nonfluctuating fluid dynamical model calculation. Then the correlation function can be evaluated using Eqs. (2)–(4).

Using the few fluid-cell sources for tests, in Ref. [10] it was shown that in the case of a globally symmetric fluid dynamical configuration the correlation function only includes $\cos(\text{const. } \mathbf{k}u_s)$ and $\cosh(\text{const. } \mathbf{k}u_s)$ terms, therefore it will not depend on the *direction* of the velocity, only on its magnitude. The *direction* dependence becomes apparent in the correlation function only if we take into account that, due to the radial expansion and the opacity of the strongly interacting QGP, the emission probability from the far side of the system is reduced compared to that from the side of the system facing the detector.

Based on the few source model results the differential HBT method was introduced by evaluating the difference of two correlation functions measured at two symmetric angles, forward and backward shifted in the reaction plane in the participant c.m. frame by the same angle, i.e., at $\eta = \pm \text{const.}$, so that the DCF becomes

$$\Delta C(k, q) \equiv C(k_+, q_{\text{out}}) - C(k_-, q_{\text{out}}). \quad (12)$$

For exactly $\pm x$ -symmetric spatial configurations (i.e., $k_{+x} = k_{-x}$ and $k_{+z} = -k_{-z}$), e.g., central collisions or spherical expansion, $\Delta C(k, q)$ would vanish! It would become finite if the rotation introduces an asymmetry.

III. FREEZE-OUT

The HBT method is sensitive to the time development of particle emission and well suited to transport models where emission happens during the ST history of the collision,

although the emission is concentrated at a FO layer. The fluid dynamical model is also able to describe emission in an ST volume or layer [12,13] or in hybrid models where a microscopic transport module is attached to the fluid dynamics (e.g., [14]). The determination of the FO surface normal or the emission direction from the ST FO layer and the emission profile in this layer are the subjects of present theoretical research (see [7] and [15–18]). This complex FO process certainly has an influence on the HBT analysis, but our present aim is not to reproduce exactly a given experiment.

We focus on a single collective effect, the rotation, developing from the angular momentum during the initial stages of the fluid dynamics. Thus we constrain our discussion to the fluid dynamical stage and adopt a relatively simple FO description from Ref. [11], which can be implemented in Eq. (10). This provides the emission weight factors, w_s , which depend on the local mean emission direction, $\hat{\sigma}^\mu$, and the flow velocity at the emission point.

The detector configuration is given by the two particles reaching a given detector in the direction of \mathbf{k} . Thus the emission weights depend on the normal of the emission surface and of the emission, i.e., $\hat{\sigma}$ and \hat{k} . Most of the particles FO in a layer along a constant proper time hyperbola, with a dominant flow four-velocity normal to this hyperbola: $\hat{\sigma}^\mu \approx u^\mu$. The origin of the hyperbola is at an ST point, which may precede the impact of the Lorentz contracted nuclei [15].

We assume in the actual numerical calculations that the expression of the weight, in Eq. (10), is the same for all surface layer elements, $Q_s^{(q)} = Q^{(q)}$ and $\Theta_s = \Theta$, so that $w_s = (k_\mu \hat{\sigma}_s^\mu) \exp(-\Theta^2 q_0^2/2)$, where $\hat{\sigma}_{s\mu} = (\sigma_s^0, \boldsymbol{\sigma}_s)$, so that $k_\mu \hat{\sigma}_s^\mu = k^0 \sigma_s^0 + \mathbf{k} \boldsymbol{\sigma}_s$. If the emission path time length, Θ , tends to 0, then the time-modifying factor becomes unity. With the choice $\hat{\sigma}_\mu = u_\mu$, the time-like FO normal is $\hat{\sigma}_{s\mu} = (\gamma_s, \mathbf{u}_s)$. Then $(k_\mu \hat{\sigma}_s^\mu) = \gamma_s k_0 + \mathbf{k}u_s$. So the weight becomes

$$w_s = (\gamma_s k_0 + \mathbf{k}u_s) \exp(-\Theta^2 q_0^2/2). \quad (13)$$

This weight is explicitly different for the mirror image cell at $\mathbf{x}_s^* \rightarrow -\mathbf{x}_s$, where $\mathbf{u}_s^* \rightarrow -\mathbf{u}_s$ and then $w_s^* = (\gamma_s k_0 - \mathbf{k}u_s) \exp(-\Theta^2 q_0^2/2)$.

The weight factors appear in both the nominator and the denominator of the correlator, so its normalization is balanced. On the other hand, the role of the different factors in the weight have an effect to determine: which cells contribute more and which cells contribute less to the integrated result.

IV. RESULTS

The sensitivity of the standard correlation function on the fluid cell velocities decreases with decreasing distances among the cells. So, with a large number of densely placed fluid cells, where all fluid cells contribute equally to the correlation function, the sensitivity on the flow velocity becomes negligibly weak.

Thus, the emission probability from different ST regions of the system is essential in the evaluation. This emission asymmetry due to the local flow velocity occurs also when the FO surface or layer is isochronous or if it happens at the constant proper time.

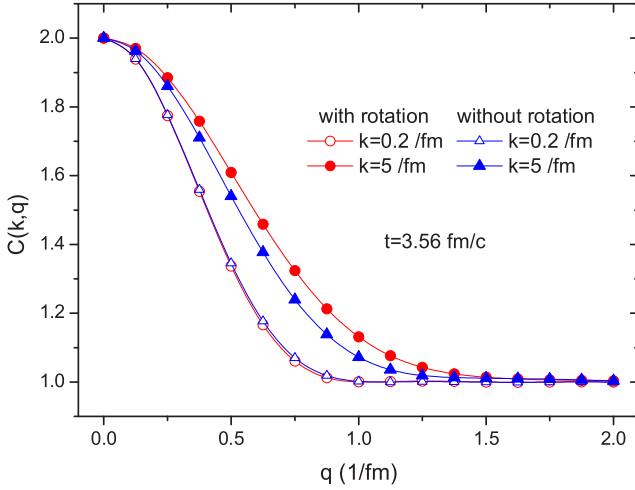


FIG. 1. (Color online) Dependence of the standard correlation function in the k_+ direction from the collective flow, at the final time, 3.56 fm/c after reaching local equilibrium and 8.06 fm/c from the first touch, including the initial longitudinal expansion Yang-Mills field dynamics [19].

We studied the fluid dynamical patterns of the calculations published in Ref. [2], where the appearance of the KHI is discussed under different conditions. We chose the configuration where both the rotation [1] and the KHI occurred at $b = 0.7b_{\max}$, with a high cell resolution and low numerical viscosity at LHC energies, where the angular momentum is large, $L \approx 10^6 \hbar$ [7].

In spatially symmetric few-source configurations [10], the standard correlation function did not show any difference when measured at two symmetric \mathbf{k} and \mathbf{q} -out angles, e.g., in the reaction $[x-z]$ plane at $\mathbf{k}_+ = (k_x, 0, +k_z)$, $\mathbf{q}_+ = (q_x, 0, +q_z)$ and $\mathbf{k}_- = (k_x, 0, -k_z)$, $\mathbf{q}_- = (q_x, 0, +q_-)$, i.e., $\Delta C(k, q)$ vanished. Here we have chosen two directions at $\eta = \pm 0.76$, that is, at polar angles of $90 \pm 40^\circ$. These are measurable with the ALICE TPC and at the ATLAS and CMS also.

The standard correlation function is influenced both by the ST shape of the emitting source and by its velocity distribution. The correlation function becomes narrower in q with increasing time, primarily due to the rapid expansion of the system. At the initial configuration the increase in $|\mathbf{k}|$ leads to a small increase in the width of the correlation function.

Nevertheless, in theoretical models we can switch off the rotation component of the flow and analyze how the rotation influences the correlation function and, especially, the DCF, $\Delta C(k, q)$. Figure 1 compares the standard correlation functions with and without the rotation component of the flow at the final time moment. Here we see that the rotation leads to a small increase in the width in q for the distribution at high values of $|\mathbf{k}|$, while at low momentum there is no visible difference.

In Fig. 2, $\Delta C(k, q)$ is shown for the configuration with and without rotation. For $k = 5/\text{fm}$ the rotation increases both the amplitude and the width of ΔC . The dependence on $|\mathbf{k}|$ is especially large at the final time.

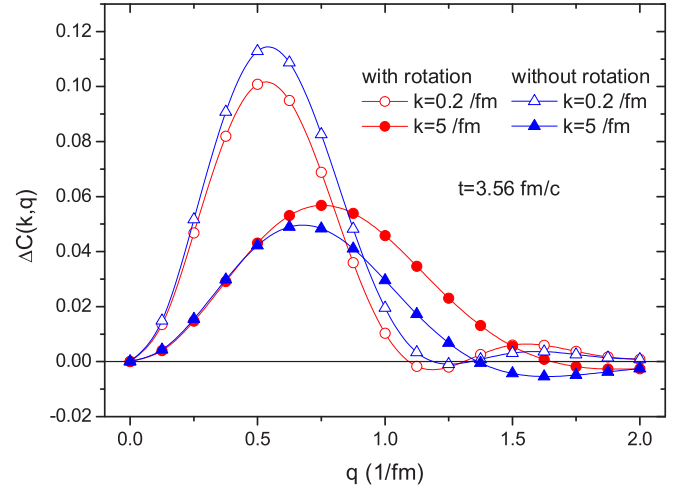


FIG. 2. (Color online) Differential correlation function, $\Delta C(k, q)$, at the final time with and without rotation.

In the original K frame defined by the beam direction and the impact parameter, we can describe the vector \mathbf{k} with coordinates, $\mathbf{k} = \begin{Bmatrix} k_x \\ k_z \end{Bmatrix}$. In the K' frame the same vector is then

$$\mathbf{k}'(\alpha) = \begin{Bmatrix} k_{x'} \\ k_{z'} \end{Bmatrix} = \begin{Bmatrix} k_x \cos \alpha - k_z \sin \alpha \\ k_z \cos \alpha + k_x \sin \alpha \end{Bmatrix}. \quad (14)$$

Then one can define the DCF,

$$\Delta C_\alpha(\mathbf{k}', \mathbf{q}'), \quad (15)$$

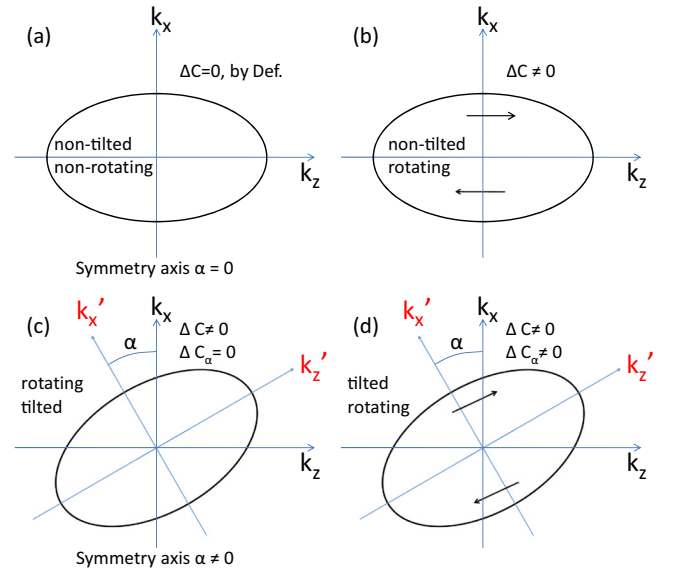


FIG. 3. (Color online) Sketch of the configuration in different reference frames, with and without rotation of the flow. The nonrotating configurations may have radial flow velocity components only. The DCF, $\Delta C_\alpha(k, q)$, is evaluated in a K' reference frame rotated by an angle α in the x, z , reaction plane. We search for the angle α , where the nonrotating configuration is “symmetric,” so that it has a “minimal” DCF as shown in Fig. 4.

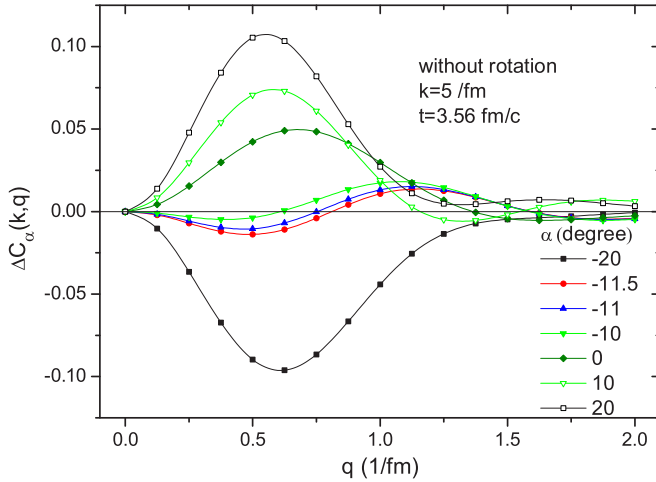


FIG. 4. (Color online) The DCF at average pion wave number $k = 5/\text{fm}$ and fluid dynamical evolution time $t = 3.56 \text{ fm}/c$, as a function of the functions of momentum difference in the “out” direction q (in units of $1/\text{fm}$). The DCF is evaluated in a frame rotated in the reaction plane, in the c.m. system, by angle α .

which depends on the angle α . We have to find the proper symmetry axes of the emission ellipsoid. The conventional way would be the standard azimuthal HBT, however, we can exploit the features of the DCF. As the analytic examples [10] show, if (i) the shape is symmetric around the x' axis, and (ii) there is no rotation in the flow, then

$$\Delta C_\alpha(\mathbf{k}', \mathbf{q}') = 0. \quad (16)$$

Thus we can use the DCF to find the angle, α' , of the proper frame K' also (Fig. 3). For a given $|\mathbf{k}|$ (e.g., $|\mathbf{k}| = 5/\text{fm}$), we search for the minimum of the norm of the DCF as a function of α .

This procedure is performed and the result is shown in Fig. 4. We separated the effect of the rotation by finding the symmetry angle where the rotationless configuration yields a vanishing or minimal ΔC for a given transverse momentum k . The figure shows the result where the rotation component of the velocity field is removed. The DCF shows a minimum in its integrated value over q , for $\alpha = -11^\circ$. The shape of the DCF changes characteristically with the angle α . Unfortunately, this is not possible experimentally, so the direction of the symmetry axes should be found with other methods, like global flow analysis and/or azimuthal HBT analysis. To study the dependence on the angular momentum the same study was done for lower angular momenta also, i.e., for lower (RHIC) energy Au + Au collisions at the same impact parameter and time. We identified the angle where the rotationless DCF was minimal, which was $\alpha = -8^\circ$, less than the deflection at a higher angular momentum.

We did this for two energies, Pb + Pb/Au + Au at $\sqrt{s_{NN}} = 2.36/0.2 \text{ TeV}$ respectively, while all other parameters of the collision were the same. The deflection angle of the symmetry axis was $\alpha = -11^\circ/-8^\circ$, respectively.⁴ In these

⁴The negative angles arise from the fact that our model calculations predict rotation, with a peak rotated forward [1].

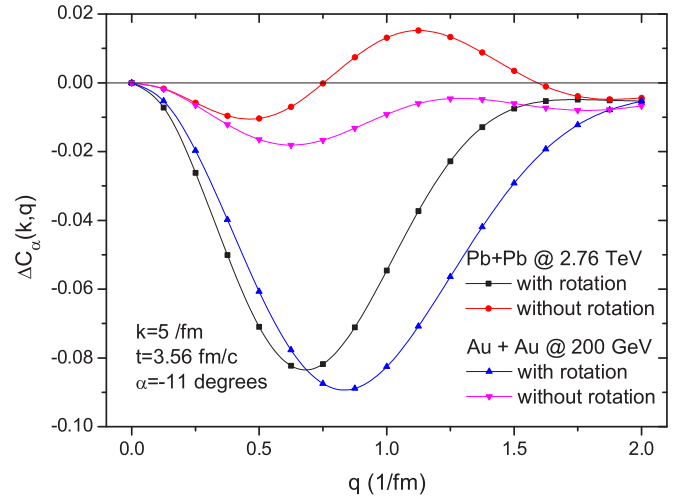


FIG. 5. (Color online) The DCF with and without rotation in the reference frames, deflected by the angle α , where the rotationless DCF is vanishing or minimal. In this frame the DCF of the original, rotating configuration indicates the effect of the rotation only. The amplitude of the DCF of the original rotating configuration doubles for the higher energy (higher angular momentum) collision.

deflected frames we evaluated ΔC for the original, rotating configurations, which are shown in Fig. 5. This provides an excellent measure of the rotation.

On the other hand, the rotationless configuration cannot be generated from experimental data in an easy way. Other methods like global flow tensor analysis and azimuthal HBT analysis [20] can provide an estimate for finding the deflection angle α .

V. CONCLUSION

The analyzed model calculations show that differential HBT analysis can give a good quantitative measure of the rotation in the reaction plane of a heavy-ion collision. These studies show that this measure is proportional to the beam energy or total angular momentum (while the polarization [4] is not). It shows the best sensitivity at higher collective transverse momenta.

To perform the analysis in the rotationless symmetry frame one can find the symmetry axis the best with the azimuthal HBT method, which provides even the transverse momentum dependence of this axis [20]. It is also important to determine the precise event-by-event c.m. position of the participants [21] and minimize the effect of fluctuations to be able to measure the emission angles accurately, which is crucial in the present $\Delta C(k, q)$ studies.

ACKNOWLEDGMENTS

This work was supported in part by the Helmholtz International Center for FAIR. We thank F. Becattini, M. Bleicher, G. Graef, P. Huovinen, and J. Manninen for comments.

- [1] L. P. Csernai, V. K. Magas, H. Stöcker, and D. D. Strottman, *Phys. Rev. C* **84**, 024914 (2011).
- [2] L. P. Csernai, D. D. Strottman, and C. Anderlik, *Phys. Rev. C* **85**, 054901 (2012).
- [3] L. P. Csernai, V. K. Magas, and D. J. Wang, *Phys. Rev. C* **87**, 034906 (2013).
- [4] F. Becattini, L. P. Csernai, and D. J. Wang, *Phys. Rev. C* **88**, 034905 (2013).
- [5] Sz. Horvát, V. K. Magas, D. D. Strottman, and L. P. Csernai, *Phys. Lett. B* **692**, 277 (2010).
- [6] B. McInnes and E. Teo, *Nucl. Phys. B* **878**, 186 (2014).
- [7] V. Vovchenko, D. Anchishkin, and L. P. Csernai, *Phys. Rev. C* **88**, 014901 (2013).
- [8] W. Florkowski, *Phenomenology of Ultra-relativistic Heavy-Ion Collisions* (World Scientific, Singapore, 2010).
- [9] A. N. Makhlin and Yu. M. Sinyukov, *Z. Phys. C* **39**, 69 (1988); S. V. Akkelin and Y. M. Sinyukov, *ibid.* **72**, 501 (1996); T. Csörgő, S. V. Akkelin, Y. Hama, B. Lukács, and Y. M. Sinyukov, *Phys. Rev. C* **67**, 034904 (2003).
- [10] L. P. Csernai and S. Velle, [arXiv:1305.0385v2](https://arxiv.org/abs/1305.0385v2) [nucl-th].
- [11] T. Csörgő, *Heavy Ion Phys.* **15**, 1 (2002).
- [12] E. Molnár, L. P. Csernai, V. K. Magas, Zs. I. Lazar, A. Nyiri, and K. Tamosiunas, *J. Phys. G* **34**, 1901 (2007).
- [13] E. Molnár, L. P. Csernai, V. K. Magas, A. Nyiri, and K. Tamosiunas, *Phys. Rev. C* **74**, 024907 (2006).
- [14] Y.-L. Yan, Y. Cheng, D.-M. Zhou, B.-G. Dong, X. Cai, B.-H. Sa, and L. P. Csernai, *J. Phys. G* **40**, 025102 (2013).
- [15] D. Anchishkin, V. Vovchenko, and L. P. Csernai, *Phys. Rev. C* **87**, 014906 (2013).
- [16] Y. Cheng, L. P. Csernai, V. K. Magas, B. R. Schlei, and D. Strottman, *Phys. Rev. C* **81**, 064910 (2010).
- [17] P. Huovinen and H. Petersen, *Eur. Phys. J. A* **48**, 171 (2012).
- [18] D. Anchishkin, V. Vovchenko, and S. Yezhov, *Int. J. Modern Phys. E* **22**, 1350042 (2013).
- [19] V. K. Magas, L. P. Csernai, and D. D. Strottman, *Phys. Rev. C* **64**, 014901 (2001); *Nucl. Phys. A* **712**, 167 (2002).
- [20] M. A. Lisa, N. N. Ajitanand, J. M. Alexander *et al.*, *Phys. Lett. B* **496**, 1 (2000); M. A. Lisa, U. Heinz, and U. A. Wiedemann, *ibid.* **489**, 287 (2000); E. Munt, G. Graef, M. Mitrovski, M. Bleicher, and M. A. Lisa, *Phys. Rev. C* **84**, 014908 (2011); G. Graef, M. Bleicher, and M. Lisa, *ibid.* **89**, 014903 (2014).
- [21] L. P. Csernai, G. Eyyubova, and V. K. Magas, *Phys. Rev. C* **86**, 024912 (2012).